Layer-by-Layer Self-Assembly of a Metallo-Supramolecular Coordination Polyelectrolyte Studied by Infrared Spectroscopy, Microgravimetry, and X-ray Reflectance

Dirk G. Kurth*, Markus Schütte
Max-Planck-Institute of Colloids and Interfaces
D-14424 Potsdam (Germany)

SUMMARY: Layer-by-Layer self-assembly on planar substrates of a Fe(II) metallo-supramolecular coordination polyelectrolyte (MEPE) and poly-(styrene sulfonate) (PSS) is investigated with a variety of surface sensitive techniques. Results from reflection-absorption infrared (RAIR) spectroscopy and microgravimetry are in agreement with linear multilayer build-up. Furthermore, RAIR spectroscopy indicates close to complete counter ion exchange during polyion deposition. The multilayers contain approximately 20 mass-percent water under ambient conditions. Water uptake and loss is completely reversible. Annealing to 250 °C in air does not affect the structural integrity of the film as demonstrated by XRR measurements.

Introduction

The design of functional and nanotechnological devices will most likely rely on bottom-up principles involving molecular self-organization.[1)] The provision of molecular components and building blocks with well-defined structures and properties is an important challenge facing modern chemistry. In addition, existing methods have to be improved and new strategies have to be developed that permit integration of molecule-based devices into macroscopic architectures.

As far as photo- and electroactive functions are concerned, much attention has been devoted to the construction of metallo-supramolecular assemblies. Bipyridine ligands in combination with second and third transition row metal ions, in particular Ru(II) and Os(II), possess promising excited-state and redox properties.[2)] But also first transition row metal ions, especially Fe(II), show exciting possibilities due to thermally or optically induced spin-transitions.[3)] In terms of structure, the use of bipyridine as ligand is not ideal for two reasons: First, stereo and/or geometric isomers are present because bidentate ligands give rise to stereoisomerism in octahedral complexes and in

 CCC 1022-1360/00/$ 17.50+.50/0

the presence of a substitutent, two geometric isomers with facial or meridional geometry can be formed. Second, building self-assembled species occurs with no stereochemical control if ligands with a substitutent are used.[4] In case of polynuclear assemblies this approach results in randomly coiled macromolecules.[5]

From geometric considerations terpyridine based ligands are much more convenient because they form stereochemically non-ambiguous complexes. Substitution in the 4' position does not cause isomerism and offers the possibility to design metallo-supramolecular assemblies in which the constituents lie in a clearly defined direction. The draw back of terpyridine ligands is their shorter excited-state life time and a weaker luminescence of the corresponding Ru(II) and Os(II) complexes. However, these disadvantages can at least in part be overcome by using suitably derivatized terpyridines[6] or other metal ions.[7]

Based on the structural advantage of terpyridine ligands we investigate polynuclear assemblies by using back-to-back terpyridines. In case of kinetically labile metal ions, such as first transition row elements, self-assembly occurs spontaneously at ambient conditions. The coordinative bond of these metal ions with terpyridine is sufficiently strong to yield extended structures, yet reversible enough to be responsive and to yield thermodynamic equilibrium structures. In principal, it is possible to change the macroscopic properties of such non-covalent polymers by an external chemical (pH, solvent etc.) or physical (shear, temperature etc.) stimulus.[8-9] Metal ion mediated self-assembly of 1,4-bis(2,2′:6′,2′′-terpyridine-4′-yl)benzene in aqueous solution results in formation of a linear, rigid-rod type macromolecule. Due to the positive charge we call these assemblies polyelectrolytes.

Recently, we showed that thin films of MEPE on planar[10] and colloidal[11] surfaces can be fabricated with the Layer-by-Layer (LbL) self-assembly method. The sequential nature of this methodology allows incorporating MEPEs with different metal ions in multilayer architectures.[12] The LbL methodology relies primarily on electrostatic interactions of the oppositely charged components and permits facile fabrication of multilayer structures with nanometer thickness control.[13]

The positive charge can also be used to self-assembly MEPE and oppositely charged amphiphiles as a means to tailor the surface chemical properties of MEPEs including solubility and surface activity. The resulting polyelectrolyte–amphiphile complex (PAC) is hydrophobic, dissolves in

common organic solvents, spreads at the air-water interface, and forms anisotropic Langmuir-Blodgett (LB) layers.[14] Our strategy combines colloidal, metallo-supramolecular, and surface chemistry and provides extensive control over structure and function at every level of the architecture.

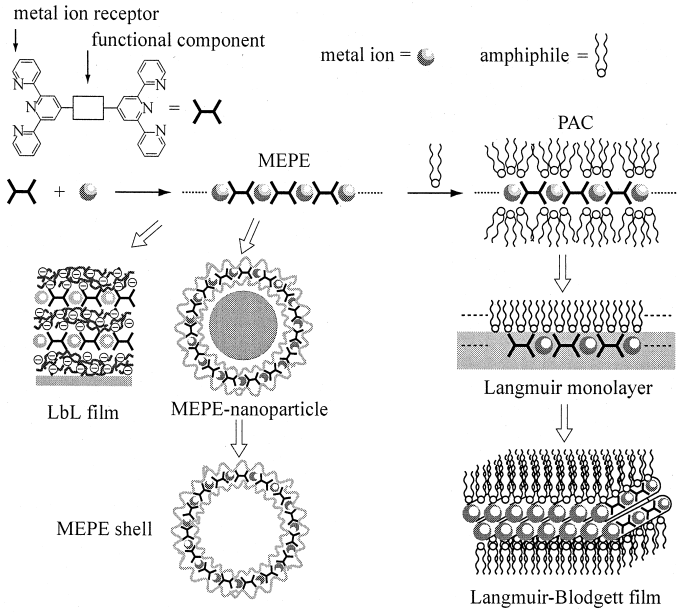

Scheme 1. Metal ion mediated self-assembly of ditopic terpyridine ligands results in MEPEs. Due to the positive charge of MEPE it is possible to fabricate ordered, macroscopic architectures by LbL on planar or colloidal substrates. Self-assembly of MEPE and amphiphiles results in PACs that are soluble in common organic solvents, form Langmuir monolayers and anisotropic LB multilayers. In principal it is possible to introduce additional functional components in the 4'-positions of the terpyridines or into the amphiphilic component. The combination of colloidal, supramolecular, and surface chemistry provides extensive control of structure and function at every level of the architecture.

Here, we use infrared spectroscopy to elucidate structural aspects of these LbL multilayers. The thermal stability of the layers is investigated by X-ray reflectance (XRR). Finally, water content, as well as in-situ water up-take and loss is measured by gravimetric analysis using quartz crystal resonators.

Results and Discussion

Investigations by Infrared Spectroscopy. Infrared spectroscopy is a wide spread non-destructive surface analytical tool, which provides information about the composition, orientation, and quantity of an adsorbate. The RAIR spectra to be discussed in the following are recorded from gold-coated substrates because of the inertness and the high reflectivity in the infrared region. To create a negatively charged, air-stable interface, the gold substrate is rendered hydrophilic by adsorption of a monolayer of mercaptopropionic acid (MPA). Then a layer of poly-(ethylenimine) (PEI) is adsorbed on the carboxylic acid derivatized gold surface. The surface confined carboxylic acid groups promote adhesion for the subsequent layer of PEI through hydrogen bonds, amide formation, and electrostatic interactions. Subsequent deposition of a layer of PSS results in a negatively charged interface.

Transmission IR-spectra of $Fe(OAc)_2$ and NaPSS as well as RAIR spectra of a film consisting of 10 (PSS/MEPE) layer pairs and a neat MEPE film are shown in Figure 1. The last sample (d) is prepared by droplet evaporation of a methanolic MEPE solution on the gold-coated substrate.

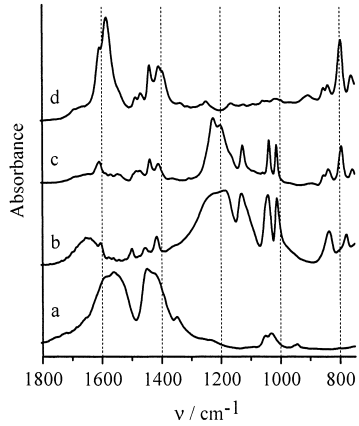

Fig. 1: Transmission infrared spectra of $Fe(OAc)_2$ (a), NaPSS (b) and RAIR spectra of $MPA/PEI(PSS/MEPE)_{10}$ (c) and neat MEPE (d) on gold coated substrates (normalized spectra reported in absorbance).

The positions of absorption bands in RAIR spectra can be compared directly. However, due to optical effects there can be differences in the band positions between transmission and RAIR

spectra.[15-16] The positions of the PSS bands are, therefore, shifted by approximately 3 cm^{-1} in the RAIR spectrum. A summary of peak positions and assignments is summarized in Table 1. Neat MEPE (d) shows several pyridine and phenyl ring breathing modes between 1610 and 1400 cm^{-1} that are, however, covered by the strong acetate bands as a comparison with the spectrum of $Fe(OAC)_2$ (a) shows. The absence of the strong acetate peaks in the RAIR spectrum of the MEPE/PSS multilayer (c) demonstrates that there are no acetate counter ions in the multilayer. This result is also confirmed by X-ray photoelectron spectroscopy (XPS).[17] Likewise, we can rule out formation of sulfonic acid during layer build-up. The $-SO_3H$ group has stretching modes at 1350 and 1172 cm^{-1} and a characteristic in-plane C=C mode due to $-C_6H_4SO_3H$ at 1097 cm^{-1}, which are clearly absent in spectrum (c).

Table 1: Prominent infrared peak positions and assignments of PSS and MEPE.[18]

Position [cm^{-1}]	Comments
$Fe(OAc)_2$	
1550	asym COO^- (vs, broad)
1460	asym. deformation mode CH_3 (m)
1450	sym COO^- (vs, broad)
1350	sym. deformation mode CH_3 (m)
MEPE	
1605	ring breathing mode
1571	ring breathing mode (strong through conjugation)
1485	ring breathing mode
1435	ring breathing mode
853 - 735	CH out of plane deformation modes (phenyl and pyridine rings)
PSS[19]	
2925	asym. CH stretch (PSS)
2850	sym. CH stretch (PSS)
1647	scissoring mode H_2O
1601, 1498, 1413	combination & overtone modes out-of-plane CH bending (phenyl ring)
1450	in-plane bending $-CH_2-$
1232, 1180	degenerated anti-sym. SO_3^- stretch (influenced by cation)
1128	in-plane CC deformation mode of $-C_6H_4-SO_3^-$
1040	sym. SO_3^- stretch (not influenced by cation)
1008	in-plane CH bending of $-C_6H_4-SO_3^-$
835	SO stretch
776	out-of-plane CH (pairs) bending (phenyl)
676	out-of-plane CH (four) bending (phenyl)

From the position of the sulfonate group in the RAIR spectrum we can draw conclusions about the nature of the counter ion.[20] Unperturbed sulfonate has three identical S–O bonds and C_{3v}-symmetry, which results in a doubly degenerated anti-symmetric stretching vibration at 1172 cm^{-1}. An electrostatic field induced by a counter anion removes the degeneracy, which results in a doublet. The splitting of the doublet increases with the strength of the electric field generated by the cation. For Na^+ as cation the splitting is 38, for Co^{2+} 77, and for Fe^{3+} 130 cm^{-1}, respectively. In the MEPE/PSS multilayer the sulfonate bands are located at 1197 and 1223 cm^{-1}.[19] The small splitting of 26 cm^{-1} is attributed to the presence of the (large) MEPE polycation. Apparently, the bulky terpyridine groups that coordinate around Fe^{2+} in an octahedral fashion shield the charge of the central cation. The symmetric stretching mode of the sulfonate group at 1036 cm^{-1} is hardly affected by the counter ion. Also, we note that the bandwidth in the RAIR spectrum of the MEPE/PSS multilayer is markedly reduced compared to the transmission spectrum. The width of the bands at 1036 and 1011 cm^{-1} are 11 and 9 cm^{-1}, while in solid PSS (b) they are 25 and 16 cm^{-1}, respectively. Inhomogeneous band broadening mechanisms are caused by perturbations associated with molecular interactions.[21] Apparently, such interactions are diminished in the MEPE/PSS multilayer, possibly because of the compound composition, which moderates direct PSS–PSS interactions.

In Figure 2, RAIR spectra of a series of multilayers $(PSS/MEPE)_n$ (n = 1, 2, 3, 4, 5, 10) on gold coated substrates are shown. The inset in Figure 2 shows the absorbance at different wave numbers as a function of the number of layers. The RAIR data clearly demonstrate linear film build-up.

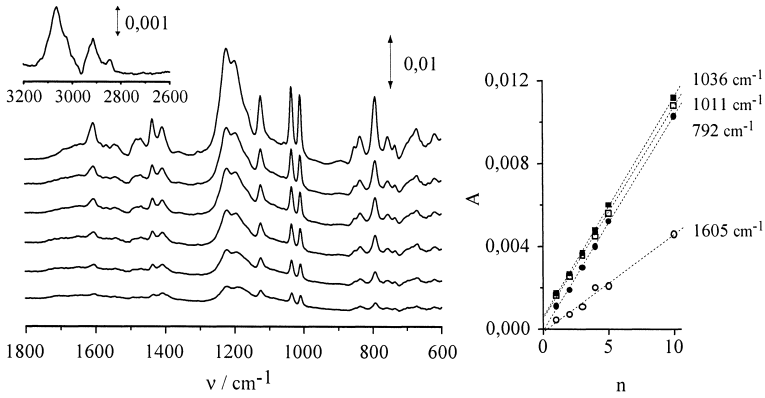

Fig. 2: Reflection-absorption infrared spectra of MPA/PEI(PSS/MEPE)$_n$ (n = 1,2,3,4,5,10) multilayer on gold coated substrates (reported in absorbance). The graph on the right shows the absorbance at selected wavelengths indicated on the right hand side of each individual plot as a function of the number of layers demonstrating linear film growth. The water absorbance and the CH-stretching modes are shown in the inset on the left (n = 10).

Also shown in Figure 2 (inset) is the region from 2600 to 3200 cm^{-1} (n = 10). The band at 3046 cm^{-1} is assigned to water that is adsorbed in the multilayer, while the bands around 2850 and 2925 cm^{-1} are assigned to the CH-stretching modes. The aromatic CH-stretching modes above 3000 cm^{-1} are masked by the water absorbance.

Thermal stability. That PSS/MEPE multilayers are thermally quite stable is demonstrated by XRR. Figure 3 shows XRR curves of a MPA/PEI/PSS(PAH/PSS)$_4$(MEPE/PSS)$_5$ multilayer on a silicon wafer that was heated to different temperatures. The occurrence of Kiessig fringes in all reflectance curves demonstrates that the multilayer thickness remains uniform after annealing. The absence of Bragg reflexes in the XRR-curves, which would indicate an internal structure, can have two reasons. Individual layers can interpenetrate, which will smear out the electron density contrast or the electron density contrast between PSS and MEPE is simply not large enough. The question concerning the internal architecture of these LBL films awaits further investigations. The film thickness becomes slightly smaller as indicated by the shift of the fringes toward smaller angles. The reflectance curves are fitted with a two-box model. To allow a smooth transition between each layer a surface roughness is introduced. Initially, the film thickness is 21.1 nm, after heating to 100 °C it is 20.7 nm and finally after heating to 250 °C it is 19.5 nm, respectively.

The reduction in film thickness is attributed to a loss of water upon annealing as will be discussed in the next section. The interfacial roughness changes slightly from 0.8 nm to 0.7 nm to 0.65 nm, respectively.

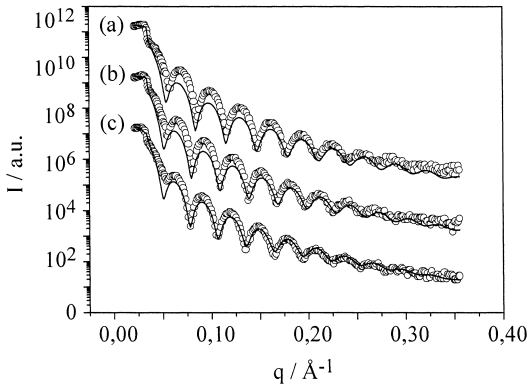

Fig. 3: XRR curves of a MPA/PEI/PSS(PAH/PSS)$_4$(MEPE/PSS)$_5$ multilayer on silicon at room temperature (a), after annealing at 100 °C for 2 hours (b) and at 250 °C for 2 hours (c). The solid lines represent calculated reflectance fits.

Investigations with the Quartz Crystal Microbalance (QCM). Measurements with the QCM provide very accurate data on mass loading in each deposition step during LbL film build-up and represent a complementary method to optical techniques, such as absorption spectroscopy. In order to prepare the QCM for LbL deposition, the gold-coated crystal was treated with MPA, PEI, and PSS as described above. For the following experiments, the QCM was alternatingly dipped into solutions containing MEPE or PSS. After each deposition step the QCM was rinsed in water, dried with a stream of argon, and data acquisition was started. In Figure 4, the frequency change, Δf, is shown as a function of the number of deposited layers. The mass loading is computed with the Sauerbrey equation.[22)]

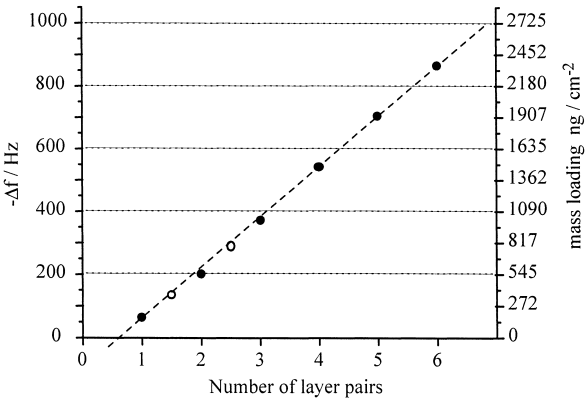

Fig. 4: Frequency change, Δf, of the QCM-resonator (9 MHz) and the corresponding mass loading as a function of the number of layers for MPA/PEI(PSS/MEPE)$_n$PSS$_m$ (n = 1 - 6, m = 0 filled circles, n = 1,2, m = 1 open circles). The dotted line is a linear curve fit.

The mass loading increases linearly with the number of layers and is in qualitative agreement with the RAIR data. The linear regression (dotted line) does not go through the origin because of the underlying MPA and PEI layers. The frequency change of a single MEPE layer is 87 Hz or 237 ng / cm^2. Similarly, deposition of a single PSS layer gives rise to a frequency change of 83 Hz, corresponding to a mass of 227 ng / cm^2. The mass loading can be converted into a layer thickness if the density of the layer is known. As an approximation for the density of the layers we use the known bulk densities of the materials. With a density of 1.5 g / cm^3 the thickness of a single MEPE layer is 2.0 nm. Likewise the PSS thickness is 1.5 nm with density of 1.2 g / cm^3.[23] These results are in agreement with previous results based on surface plasmon resonance spectroscopy.[24]

When it comes to device performance, knowledge of the amount of water adsorbed is of paramount importance. The QCM allows determining the up-take and loss of water in films in-situ. For the following measurements a multilayer with the composition MPA/PEI(PSS/MEPE)$_6$ is alternatingly exposed to dried or water saturated air. The change in resonance frequency of the coated QCM-crystal is shown in Figure 5. If the crystal is exposed to water saturated air the frequency drops as a result of water adsorption and reaches a plateau within a few minutes. Likewise, exposure to dry air results in a frequency increase of the QCM-resonantor due to desorption of water. The time response of the resonance frequency does not reflect the kinetics of water ad-

sorption and desorption but also contains contributions from equilibration in the QCM sample chamber. The resonance frequency change is completely reversible and amounts to approx. 210 Hz, which corresponds to a mass loading of 570 ng / cm^2. The total uptake of water is approx. 20% of the total mass loading. For comparison, a multilayer composed of PSS/PAH shows a water uptake of 18%. These data are in agreement with the data reported by others[25] and indicate that water uptake in these polyelectrolyte films is substantial.

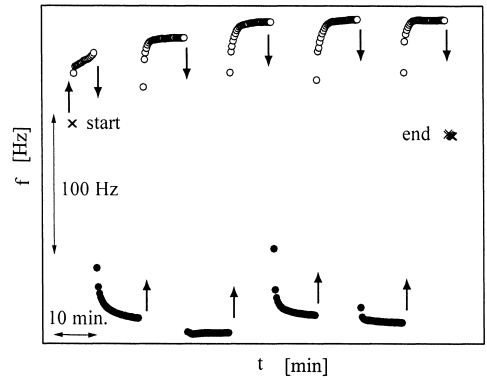

Fig. 5: Resonance frequency, *f*, of a QCM coated with a MPA/PEI(PSS/MEPE)$_6$ multilayer exposed alternatingly to dry or water saturated air. The data points labeled "start" and "end" are the frequencies at ambient conditions before and after the experiment. Open circles correspond to dry and filled circles to water saturated air, respectively.

Experimental

MEPE was synthesized and layers were fabricated according to previously published procedures.[9]

Infrared spectra were recorded with a Bruker Equinox 55/S Fourier Transform Spectrometer equipped with a liquid nitrogen cooled MCT-detector for reflection-absorption measurements and a DTGS detector for transmission spectra. For transmission spectra the material was thoroughly mixed with dried KBr and pressed to a transparent pellet. RAIR spectra were recorded with evaporated gold-on-glass substrates with a modified commercial reflection setup (Harrick) using a static linear polarization modulation protocol described elsewhere.[26] A total of 200 scans were

accumulated; the polarization of the incoming beam was switched from parallel to perpendicular every 20 scans.

QCM-measurements were performed with a HP-53131 frequency counter, a HP-4194A impedance analyzer, and a custom-made resonator circuit powered by a HP-E3620A power supply. Data acquisition was carried out with a PC computer interfaced via HP Visual Basic to the frequency counter. Mass changes were calculated from the Sauerbrey equation, the applicability of which was confirmed by impedance analysis.[27] Measurements were performed in an air-conditioned laboratory at 22 °C. The QCM was first dipped in a solution containing MPA (1 mM, Ethanol), PEI (1mM, water), poly-(allylamine hydrochloride) (PAH) (1mM) for 20 minutes. The crystal was rinsed with water and dried with a stream of pressurized air. The crystal was mounted in the sample chamber, equilibrated for 10 minutes and then measurements were taken for 3 min with 1 s intervals. Final frequency readings were stable within ±1 Hz. Measurements were done with the QCM sample chamber being at ambient conditions, filled with KOH or with water saturated cotton.

XRR experiments were performed with a commercial instrument (STOE & CIE GmbH, Darmstadt, Germany) using 1.54 Å radiation. Analysis of the XRR data was performed with a box-model simulation using standard electrodynamic theory of stratified media.[28] The following parameters were used: Film: $\delta\, 4{\cdot}10^{-6}\ \beta\, 0$, substrate $\delta\, 8.875{\cdot}10^{-6}\ \beta\, 1{\cdot}10^{-7}$.

Conclusion

Layer-by-layer self-assembly of MEPE with PSS is investigated by RAIR spectroscopy and QCM measurements. The RAIR and QCM data are in agreement with linear multilayer build-up and confirm our previously published results.[8, 20] Within the sensitivity of RAIR spectroscopy, no acetate counter ions are found in the multilayer assembly. Likewise, the reduced splitting of the SO-stretching modes in the MEPE/PSS multilayer supports ion exchange of Na^+ with a less polarizing ion, presumably the MEPE-polycation. These data suggest a close to complete counter ion exchange. The PSS vibrational modes are considerably narrowed in the multilayer, which is attributed to the composite architecture of the multilayers. Annealing to 250 °C in air does not af-

fect the structural integrity of the film. These multilayers can contain up to 20 mass-percent water under ambient conditions. Water uptake and loss is completely reversible.

On-going experiments with different metal ions and ditopic ligands lead us to assume that this approach should be of general utility to immobilize metallo-supramolecular coordination polyelectrolytes on planar or colloidal substrates. Among those, terpyridine and first transition row metal ions with their well-defined octahedral coordination geometry, electrochemistry, magnetic, and electronic spin state switching properties are very promising candidates for the construction of functional devices with well-defined structures and predictable properties. Layering different components offers opportunities to fabricate films with vectorial transport properties. Further work to explore the properties of these MEPE and PAC assemblies in the volume phase and in thin films is in progress.

Acknowledgement

Valuable discussions with H. Möhwald are gratefully acknowledged. The authors thank C. Stolle for her help in the preparation of the compounds.

References

1. D. Volkmer, A. Du Chesne, D. G. Kurth, H. Schnablegger, P. Lehmann, M. J. Koop, A. Müller, *J. Am. Chem. Soc.*, **122**, 1995 (2000).
2. R. Ziessel, M. Hissler, A. El-ghayoury, A. Harriman, *Coord. Chem. Rev.* **178-180**, 1251 (1998).
3. P. Gütlich, A. Hauser, H. Spiering,. *Angew. Chem. Int. Ed.* **33**, 2024 (1994).
4. E. C. Constable, A. M. W. C. Thompson, *J. Chem. Soc. Dalton Trans.* 3467 (1992).
5. R. Knapp, A. Schott, M. Rehahn, *Macromolecules*, **29**, 479 (1996).
6. M. Maestri, N. Armaroli, V. Balzani, E. C. Constable, A. M. W. C. Thompson *Inorg. Chem.* **34**, 2759 (1995).
7. N. W. Alcock, P. R. Barker, J. M. Haider, M. J. Hannon, C. L. Painting, Z. Pikramenou, E. A. Plummer, K. Rissanen, P. Saarenketo *J.Chem. Soc. Dalton Trans.* **9**, 1447 (2000).
8. A. Aggeli, M. Bell, N. Boden, J. N. Keen, P. F. Knowles, T. C. B. McLeish, M. Pitkeathly, S. E. Radford, *Nature* **386**, 259 (1997).
9. N.Yamaguchi, H. W.Gibson *Angew. Chem. Int. Ed.* **38**,143 (1999).
10. M. Schütte, D. G. Kurth, M. R. Linford, H. Cölfen, H. Möhwald, *Angew. Chem. Int. Ed.* **37**, 2891 (1998).
11. D. G. Kurth, F. Caruso, C. Schüler *Chem. Commun.* 1579 (1999).
12. D. G. Kurth, M. Schütte, J. Radnik, to be published elsewhere.
13. G. Decher, M. Eckle, J. Schmitt, B. Struth, *Curr. Opin. Coll. Interf. Sci.* **3**, 32 (1998).
14. D. G. Kurth, P. Lehmann, M. Schütte, *Proc. Natl. Acad. Sci. USA* **97**, 5704 (2000).
15. D. G. Kurth, T. Bein, *Langmuir* **11**, 578 (1995).
16. J. F. Kang, D. G. Kurth, A. Ulman, R. Jordan, *Langmuir* **15**, 5555 (1999).
17. D. G. Kurth, M. Schütte, to be published elsewhere.
18. K. Naknishi, P. H. Solomon, *Infrared Absorption Spectroscopy*, 2nd Ed., Holden-Day, San Francisco 1977.
19. G. Zundel, *Hydration and Intermolecular Interactions*, Academic, New York 1969.
20. H. Wang, C. K. Mann, J. T. Vickers, *Appl. Spectrosc.* **49**, 127 (1995).
21. D. Steele, J. Yarwood (Ed.) In *Spectroscopy and Relaxation of Molecular Liquids*, Elsevier, Amsterdam 1991.
22. G. Sauerbrey, *Z. Phys.* **155**, 206 (1959).
23. Y. Lvov, K. Ariga, M. Onda, I. Ichinose, T. Kunitake *Coll. Surf. A.* **146**, 337 (1999).
24. D. G. Kurth, R. Osterhout *Langmuir* **15**, 4842 (1999).
25. T. Farhat, G. Yassin, S. T. Dubas, J. B. Schlenoff, *Langmuir* **15**, 6621 (1999).
26. D. G. Kurth, *Langmuir* **14**, 6987 (1998).
27. D. A. Buttry, M. D. Ward, *Chem. Rev.* **92**, 1355 (1992).
28. A. Asmussen, H. Riegler, *J. Chem. Phys.*, *104*, 8159 (1996); b) Electron densities were taken from: T. P. Russel *Materials Science Reports 5*, 171 (1990).